PHOTONIC SENSORS / Vol. 4, No. 3, 2014: 248–253

Two-Dimensional Photonic Crystal Based Sensor for Pressure Sensing

Krishnan VIJAYA SHANTHI* and Savarimuthu ROBINSON

PG Scholar, Communication Systems, Mount Zion College of Engineering and Technology, Pudukkottai-622507, Tamil Nadu, India

*Corresponding author: Krishnan VIJAYA SHANTHI Email: shanthi.krish91@gmail.com

Abstract: In this paper, a two-dimensional photonic crystal (2DPC) based pressure sensor is proposed and designed, and the sensing characteristics such as the sensitivity and dynamic range are analyzed over the range of pressure from 0 GPa to 7 GPa. The sensor is based on 2DPC with the square array of silicon rods surrounded by air. The sensor consists of two photonic crystal quasi waveguides and L3 defect. The L3 defect is placed in between two waveguides and is formed by modifying the radius of three Si rods. It is noticed that through simulation, the resonant wavelength of the sensor is shifted linearly towards the higher wavelength region while increasing the applied pressure level. The achieved sensitivity and dynamic range of the sensor is 2 nm/GPa and 7 Gpa, respectively.

Keywords: Photonic crystal, waveguide, photonic band gap, optical sensor, FDTD method pressure sensor

Citation: Krishnan VIJAYA SHANTHI and Savarimuthu ROBINSON, "Two-Dimensional Photonic Crystal Based Sensor for Pressure Sensing," *Photonic Sensors*, 2014, 4(3): 248–253.

1. Introduction

In 1987, Eli Yablonovitch and Sajeev John published their research work on photonic crystals, predicting the existence of the photonic band gap as well as the potential for inhibiting spontaneous emission and localizing light within defects in a periodic lattice of appropriate dimensions [1].

The photonic crystal is composed of periodic dielectric or metallo-dielectric nanostructures that have alternate low and high dielectric constant materials (refractive index) to affect the propagation of electromagnetic waves inside the structure. By introducing the point and/line defects inside the structure, it is possible to localize the light in the photonic bandgap (PBG) region [2].

The classifications of photonic crystals (PCs) are one-dimensional photonic crystal (1DPCs), two-dimensional photonic crystals (2DPCs), and three-dimensional photonic crystals (3DPCs). The sensor, based on 2DPCs, is receiving increasing attention from the scientific community because it has relatively simple structure, small size, better confinement of light, accurate band gap calculation, and easy integration compared to 1DPCs and 3DPCs [2].

The optical sensor is an analytical device, used to convert the amount of analytes into a detectable signal, also used for sensing applications like industrial process control, military, environment monitoring, and medical diagnostic. It relies upon a phenomenon called the evanescent field to monitor changes in the refractive index occurring within a few hundred nanometers of the sensor surface. Typically, there are two approaches reported for

Received: 21 April 2014 / Revised version: 11 June 2014

DOI: 10.1007/s13320-014-0198-8
Article type: Regular

optical sensing namely the resonant wavelength shift scheme and intensity scheme for which the resonant wavelength shift scheme is preferred for sensing approach because the shift of the resonant wavelength leads to the high sensitivity [3, 4].

Based on above sensing mechanisms, the optical sensors have been designed and analyzed, using directional couplers [5], Mach-Zehnder interferometers [6], nano-ring resonators [4, 7–12], and micro-ring resonators [13, 14] for different applications, reported in the literature. In the literature, PC/PCRR (photonic crystal ring resonator) based sensors were reported for chemical sensing, force and strain sensing [7–12], refractive index and gas sensing [15–17], dengue virus detection [18], pressure sensing [12, 19, 20], aqueous environment [21] and biosensing (proteins, avidins, BSA, DNA, etc.) applications [22–29].

In the literature, the pressure sensor using the photonic crystal was reported periodically. In 2007, Chengkuo Lee *et al.* reported a pressure sensing based 2DPC microcavity structure and achieved a linear resonant wavelength shift according to the applied pressure from 1 MPa to 5 Mpa [20]. Bakhtazad *et al*. designed a pressure sensor based on a photonic crystal waveguide suspended over a silicon substrate. Under the applied pressure, the photonic crystal waveguide is deflected toward the substrate, causing a decrease in optical transmission due to the coupling of the waveguide field to the silicon substrate [30]. Yuerui Lu *et al*. reported an all-optical pressure sensor by fabricating controllable vertical silicon nano wire arrays on a Si/SiO_2 membrane. Applying the hydrostatic pressure bent the membrane, leading to the membrane color change due to the modulation of the nano wire pitch and deflection angle [31]. In 2012, S. Olyaee *et al*. reported a pressure sensor based on 2DPC, and it had the hexagonal lattice of air holes in Si. A waveguide was directly coupled to a nano cavity and was configured by eliminating one line of air holes for its structure with the achieved sensitivity of 11.7 nm/GPa [32]. Saeed Olyee *et al*. reported a high resolution and wide dynamic range photonic crystal pressure sensor. The designed sensor had a linear behavior between 0.1 GPa and 10 GPa of the applied pressure and the pressure sensitivity of 8 nm/GPa [19]. Xuehui Xiong *et al*. reported a two-dimensional photonic crystal based sensor which had a good linear relation between the resonant wavelength and the pressure [33]. Many PC based pressure sensors were proposed and designed, however, the reported sensor was not able to provide the higher sensitivity and larger dynamic range. In order to enhance the sensing characteristics, the L3 defect based sensor was designed and analyzed.

In this paper, a photonic crystal waveguide based pressure sensor is designed, and sensing characteristics are analyzed over the range from 0 Gpa to 7 Gpa. The sensing characteristics such as the *Q*-factor, resonant wavelength, output power, sensitivity, and dynamic range are investigated. The rest of the paper is arranged as follows. In Section 2, the structure design of the PC based pressure sensor is presented. Simulation results are analyzed in Section 3. Section 4 concludes the paper.

2. Structure design

The designed photonic crystal based pressure sensor consists of the square array of circular rods placed in a background of air. The circular rods with the square lattice structure are used for reducing the scattering loss and effectively controlling the transverse electric (TE) mode propagation. In the square lattice, the number of rods in *X* and *Z* directions is 17×21. The distance between the two adjacent rods is 540 nm which is termed as the lattice constant and denoted by *a*. The radius of the rod is 0.1 μm, and the dielectric constant of the Si rod is 11.9716 (refractive index = 3.46).

The band diagram in Fig. 1 gives the propagation modes in the PC structure, which has a PBG for TE modes whose electric field is parallel to the rod axis.

The PC structure has two TE PBGs. The first reduced PBG is ranging from 0.295 a/λ to 0.435 a/λ whose corresponding wavelength range is between 1241 nm and 1830 nm, and the second PBG is from 0.732 a/λ to 0.754 a/λ whose corresponding wavelength range is between 716 nm and 737 nm. The frequency of the PC structure is $\omega a/2\pi c = a/\lambda$, where ω is the angular frequency, a is the lattice constant, c is the velocity of light in the free space, and λ is the free space wavelength. The plane wave expansion (PWE) method is employed to estimate the band gap and propagation modes of the PC structure without and with defects. The simulation parameters of the sensor are listed in Table 1.

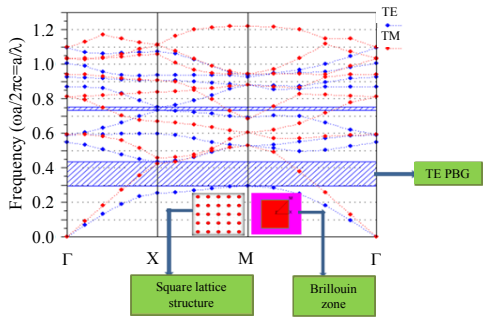

Fig. 1 Band diagram of the 1×1 photonic crystal square lattice structure.

Table 1 Parameters and its values used for sensor.

Parameters	Values
Radius of the rod	0.1 μm
Lattice constant	540 nm
Refractive index of rod	3.46
Background index	1
Size	12.4 μm × 9.2 μm (21×17 rods)
PBG range	0.295 a/λ to 0.435 a/λ (1241 nm – 1830 nm)
Polarization	TE

Figure 2 depicts the schematic diagram to sense the pressure using the 2DPC. The optical source emits the optical signal which passes to the PC based sensor. This sensor is used to manipulate light with respect to the refractive index variation of the pressure. Then, the manipulated light passes to the photodetector which is used to convert the optical light into the electrical signal. Then, the signal processing units map the sensed quantity in the readable form with the help of the look-up table which is displayed in the display board.

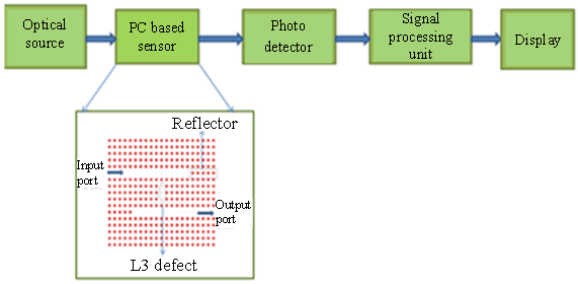

Fig. 2 Schematic structure of the PC based sensor for pressure sensing.

2.1 Sensing principle

The applied hydrostatic pressure based on the electronic and optical properties of the material such as the energy gap and refractive index can be considered for sensing applications. When a crystal is compressed by the pressure, the band gap is increased. The refractive index of Si is modified when optical coefficients such as photoelastic, piezoelectric, and permittivity changes in different pressures. In the PC structure, the PBG is dependent on the refractive index, lattice constant, and radius to lattice constant ratio r/a. By applying the pressure to the PC, the refractive index of the material, the geometrical shape of the PC, and the PBG of the structure change. In the PC waveguide coupled to the resonator output, the spectrum of the waveguide changes with different pressures. On the other hand, the resonant wavelength of the resonator is dependent on the geometrical shape of the defect that forms the cavity. By applying certain pressure to the structure, the resonant wavelength shift and intensity variation of the resonator can be measured as a function of the pressure.

Thus, the pressure-modified refractive index value reduces to

$$n = n_0 - (c_1 + 2c_2)\,\sigma \tag{1}$$

where c_1 and c_2 are defined as

$$c_1 = n_0^3\,(P_{11} - 2VP_{12}) \;/\; (2E) \tag{2}$$

$$c_2 = n_0^3\,(P_{12} - V\,(P_{11}+P_{12})) \;/\; (2E) \tag{3}$$

where n_0 is the refractive index at the zero pressure, E is Young's modulus, V is Poisson's ratio, and P_{ij} denotes the strain-optic constant.

The refractive index of the sensor increases

linearly while increasing the applied pressure. In the PC structure, an increase in the refractive index increases the resonant wavelength of the sensor shifting to the higher wavelength. It is noticed that the refractive index around 0.03985 is increased while increasing the applied pressure by 1 GPa. By combining the aforementioned principle, the sensing characteristics are analyzed. If the applied pressure is entered into the structure, the refractive index of the sensor varies according to the applied pressure, and the resonant wavelength of the sensor shifts to the higher wavelength region.

Figure 3(a) shows that the photonic crystal based pressure sensor structure has two waveguides in the *X* direction, and L3 defect is positioned between them. The input Gaussian signal is applied to the port marked "input port" with an arrow on the left side of the waveguide, and the output is detected using a power monitor at the output port marked "output port" with an arrow on the right side of the waveguide. The waveguide is formed by introducing line defects whereas the L3 defect is formed by modifying the radius of three rods by 0.03 μm. The reflector is positioned at each corner of the waveguide which is used to enhance the output power by reflection at resonance. When the defects are created in the structure, the completeness of the PBG is broken, and the guided modes (even and odd modes) propagate inside the PBG region. The guided modes are regulated by controlling the defect size and shape. Figure 3(b) shows the 3D view of the PC based pressure sensor structure. The size of the pressure sensor is 12.4 μm × 9.2 μm.

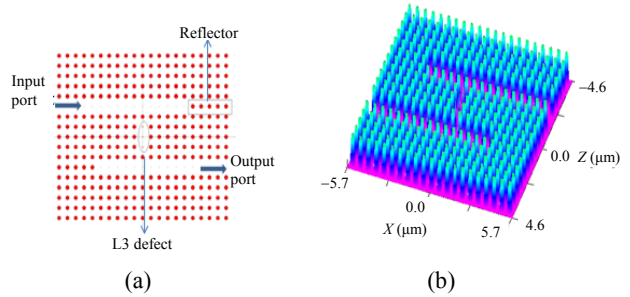

(a) (b)

Fig. 3 Photonic crystal based pressure sensor: (a) schematic diagram and (b) 3D view.

3. Simulation results

The 2D finite-difference time-domain (FDTD) method is used to investigate the performance of the sensor such as the sensitivity and dynamic range. A light signal is launched into the input port of the waveguide. The output signal is recorded by a power monitor at the output port. The output signal power from the power monitor which is positioned at the output port is normalized by the input signal power i.e., the output power is the normalized output power. The obtained output response is used to analyze the resonant wavelength, quality factor, and output power.

Figure 4 shows the normalized transmission spectrum of the sensor at the pressure of 0 Gpa. In the absence of the pressure, the resonant wavelength, *Q*-factor, and output efficiency of the sensor are 1500 nm, 75.5, and 57.5%, respectively.

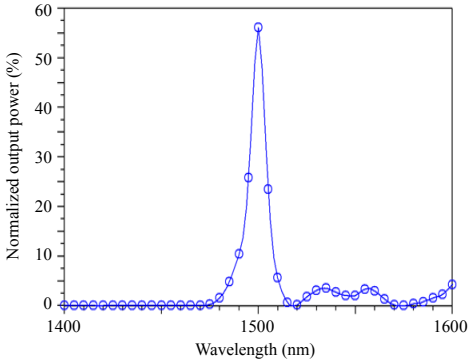

Fig. 4 Normalized transmission spectra of the sensor at 0Gpa of pressure.

Figure 5 shows the normalized output spectra of the sensor at the pressure ranging from 0 Gpa to 7 Gpa. The observed results shows that the resonant wavelength of the structure shifts to the longer wavelength while increasing the refractive index difference per Gpa of the pressure. The sensor is based on the resonant wavelength shift scheme. It is noticed that the resonant wavelength around 2 nm is obtained for every 1-GPa increase at the applied pressure. The sensitivity and dynamic range of the sensor are 2 nm/Gpa and 7 Gpa, respectively. The applied pressure with its refractive index, resonant wavelength, *Q*-factor, and output power of the

sensor between 0 Gpa and 7 Gpa are tabulated in Table 2.

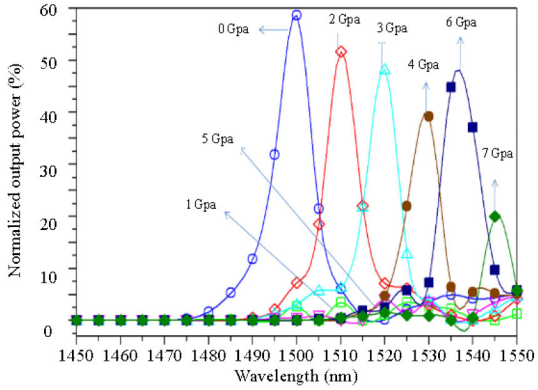

Fig. 5 Normalized transmission spectra of the sensor at the pressure of 0 Gpa to 7 Gpa.

Table 2 Analysis of the pressure with its refractive index, resonant wavelength, output power, and quality factor of the sensor at the pressure of 0 Gpa to 7 Gpa.

Level of pressure	Refractive index	Resonance wavelength (nm)	Output power (%)	*Q*-factor
0Gpa	2.50000	1500.0	57.5	75.500
1Gpa	2.53985	1530.0	3.5	153.000
2Gpa	2.57970	1510.0	55.0	151.000
3Gpa	2.61955	1520.0	50.0	152.000
4Gpa	2.65940	1525.0	13.5	52.500
5Gpa	2.69925	1530.0	40.0	255.000
6Gpa	2.73910	1535.0	49.0	153.500
7Gpa	2.77895	1545.0	20.0	772.500

Figures 6(a) and 6(b) depict the electric filed pattern of the ON-resonance and OFF-resonance of the sensor at 1500 nm and 1450 nm, respectively. At the resonant wavelength λ=1500 nm, the electric field of the waveguide is fully coupled in the L3 cavity and reaches the output port, whereas at the OFF-resonance λ=1450 nm, the signal is decoupled at the output port.

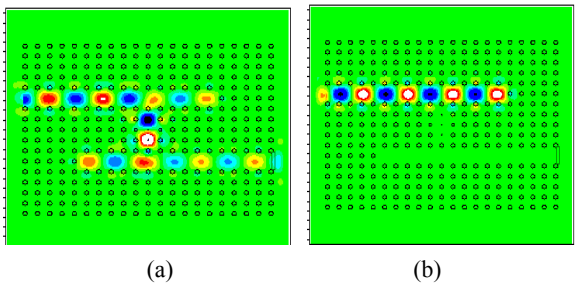

(a) (b)

Fig. 6 Electric field distribution of the sensor at (a) ON-resonance and (b) OFF-resonance.

4. Conclusions

The two-dimensional photonic crystal based pressure sensor is designed, and its sensing characteristics are analyzed. The sensor is designed using the two-dimensional photonic crystal with the square array of circular rods surrounded by air. The sensor is designed for 1450 nm to 1550 nm, which is used for the analysis of the pressure from 0 Gpa to 7 Gpa. The sensor is designed with the lattice constant a=540 nm, the radius of the rod r=100 nm, and the index difference 2.5. It is noticed that the resonant wavelength of the sensor is shifted to the longer wavelength while increasing the pressure. In the absence of the pressure, the resonance wavelength, *Q*-factor, and output power are 1500 nm, 75.5, and 57.5%, respectively. The size of the pressure sensor is 12.4 μm×9.2 μm which is highly suitable for the sensing applications.

References

[1] E. Yablonovitch, "Inhibited spontaneous emission on solid-state physics and electronics," *Physical Review Letters*, 1987, 58(20): 2059–2062.

[2] J. D. Joannopoulos, R. D. Meade, and J. N. Winn, *Photonic crystal: modeling of flow of light*. Princeton, NJ: Princeton University Press, 1995.

[3] IUPAC, *Compendium of chemical terminology*. Oxford: Blackwell Scientific Publications, 1997.

[4] C. Y. Chao and L. J. Guo, "Design and optimization of micro ring resonators in biochemical sensing applications," *Journal of Lightwave Technology*, 2006, 24(3): 1395–1402.

[5] B. J. Luff, R. D. Harris, J. S.Wilkinson, R. Wilson, and D. J. Schiffrin, "Integrated-optical directional coupler biosensor," *Optics Letters*, 1996, 21(8): 618–620.

[6] F. Prieto, B. Sepulveda, A. Calle, A. Llobera, C. Domynguez, A. Abad, *et al.*, "An integrated optical interferometric nanodevice based on silicon technology for biosensor applications," *Nanotechnology*, 2003, 14(8): 907–912.

[7] T. T. Mai, F. L. Hsiao, C. Lee, W. Xiang, C. Chenc, and W. K. Choi, "Optimization and comparison of photonic crystal resonators for silicon microcantilever sensor," *Sensors and Actuators A: Physics*, 2011, 165(1): 16–25.

[8] B. Li, F. L. Hsiao, and C. Lee, "Computational

characterization of photonic crystal cantilever sensor using hexagonal dual-nano-ring based channel drop filter," *IEEE Transactions on Nanotechnology*, 2011, 10(4): 789–796.

[9] B. Li and C. Lee "Computational study of NEMS diaphragm sensor using triple nano-ring resonator," *Procedia Engineering*, 2010, 5: 1418–1421.

[10] F. Hsiao and C. Lee, "Computational study of photonic crystals nano-ring resonator for biochemical sensing," *IEEE Sensors*, 2010, 10(7): 1185–1191.

[11] B. Li, F. L. Hsiaoa, and C. Lee, "Configuration analysis of sensing element for photonic crystal based NEMS cantilever using dual nano-ring resonator," *Sensors and Actuators*, 2011, 169(2): 352–361.

[12] B. Li and C. Lee, "NEMS diaphragm sensors integrated with triple-nano-ring resonator," *Sensors and Actuators*, 2011, 172(1): 61–68.

[13] C. Y. Chao, W. Fung, and L. J. Guo, "Polymer microring resonators for biochemical sensing applications," *IEEE Journal of Selected Topics in Quantum Electronics*, 2006, 12 (1): 134–142.

[14] S. Robinson and R. Nakkeeran, "PC based optical salinity sensor for different temperatures," *Photonic Sensors*, 2012, 2(2): 187–192.

[15] C. Kang, C. Phare, and S. M. Weiss, "Photonic crystal defects with increased surface area for improved refractive index sensing," in *Conference on Laser and Electro Optics and Quantum Electronics and laser Science*, San Jose, California, United States, May 16–21, pp. 1–2, 2010.

[16] L. A. Shiramin, R. Kheradmand, and A. Abbasi, "High-sensitive double-hole defect refractive index sensor based on 2-D photonic crystal," *IEEE Sensors*, 2013, 13(5): 1483–1486.

[17] J. Jágerská, N. L. Thomas, H. Zhang, Z. Diao, and R. Houdré, "Refractive index gas sensing in a hollow photonic crystal cavity," in *12th International Conference on Transparent Optical Networks (ICTON)*, Munich, June 27–July 1, pp. 1–4, 2010.

[18] S. Mandal, J. Goddard, and D. Erickson, "Nanoscale optofluidic sensor arrays for Dengue virus detection," in *Conference on Laser and Electro-Optics/ Conference on Quantum Electronics and Laser Science (CLEO/QELS)*, San Jose, CA, May 4–9, pp. 1–2, 2008.

[19] O. Saeed and D. A. Asghar, "High resolution and wide dynamic range pressure sensor based on two-dimensional photonic crystal," *Photonic Sensors*, 2012, 2(1): 92–96.

[20] C. Lee, J. Thillaigovindan, and R. Radhakrishnan, "Design and modeling of nanomechanical sensors using silicon 2-D photonic crystals," *Journal of Lightwave Technology*, 2008, 26(7): 839–846.

[21] F. AbdelMalek, "Design of a novel left-handed photonic crystal sensor operating in aqueous environment," *IEEE Photonics Technology Letters*, 2011, 23(3): 188–190.

[22] C. Lee, A. Sueh, P. Yee, J. L. Perera, C. Chen, and N, Balasubramanian, "Design of nanobiophotonics resonators for biomolecules detection," in *IEEE International Conference on Nano/Micro Engineered and Molecular Systems*, Sanya, January 6–9, pp. 274–279, 2008.

[23] F. Pisanello, L. Martiradonna, P. P. Pompa, T. Stomeo, A. Q. G. Vecchio, S. Sabella, *et al.*, "Parallel and high sensitive photonic crystal cavity assisted read-out for DNA-chips," *Microelectronic Engineering*, 2010, 87(5–8): 747–749.

[24] H. Kurt and D. S. Citrin, "Biochemical sensors with photonic crystals in the terahertz region," in *Conference on Lasers & Electro-Optics (CLEO)*, Atlanta, USA, May 22–27, 2005.

[25] M. R. Lee and P. M, Fauchet, "Nanoscale microcavity sensor for single particle detection," *Optics Letters*, 2007, 32(22): 3284–3286.

[26] M. R. Lee and P. M. Fauchet, "Two-dimensional silicon photonic crystal based biosensing platform for protein detection," *Optics Express*, 2007, 15(8): 4530–4535.

[27] S. C. Buswell, V. A. Wright, J. M. Buriak, V. Van, and S. Evoy, "Specific detection of proteins using photonic crystal waveguides," *Optics Express*, 16(20): 15949–15957, 2007.

[28] S. Zlatanovic, L. W. Mirkarimi, M. M. Sigalas, M. A. Bynum, E. Chow, K. M. Robotti, *et al.*, "Photonic crystal microcavity sensor for ultracompact monitoring of reaction kinetics and protein concentration," *Sensors and Actuators*, 2009, 141(1): 13–19.

[29] M. Yuna, Y. Wana, J. Lianga, F. Xiaa, M. Liua, and L. Renb, "Multi-channel biosensor based on photonic crystal waveguide and microcavities," *Optik*, 2012, 123: 1920–1922.

[30] A. Bakhtazad, J. Sabarinathan, and J. L. Hutter, "Mechanical sensitivity enhancement of silicon based photonic crystal micro-pressure sensor," in *International Symposium on Optomechatronic Technologies (ISOT)*, Toronto, October 25–27, pp. 1–5, 2010.

[31] Y. Lu and A. Lal, "Photonic crystal based all-optical pressure sensor," in *IEEE 24th International Conference on Micro Electro Mechanical Systems (MEMS)*, Cancun, January 24–27, pp. 621–624, 2011.

[32] S. Olyaee and A. A. Dehghani, "Nano-pressure sensor using high quality photonic crystal cavity resonator," in *8th International Symposium on Communication Systems, Networks & Digital Signal Processing (CSNDSP)*, Poznan, July 18–20, pp. 1–4, 2012.

[33] X. Xiong, P. Lu, and D. Liu, "Modeling of pressure sensors based on two-dimensional photonic crystalso," *Optoelectronis*, 2009, 2(2): 219–221.